

**DEGRADATION OF TRICHLOROETHYLENE USING ADVANCED
REDUCTION PROCESSES**

A Thesis

by

HAJAR FARZANEH

Submitted to the Office of Graduate and Professional Studies of
Texas A&M University
in partial fulfillment of the requirements for the degree of

MASTER OF SCIENCE

Chair of Committee,	Ahmed Abdel-Wahab
Committee Members,	Mohamed Nounou
	Eyad Masad
Head of Department,	Nazmul Karim

December 2014

Major Subject: Chemical Engineering

Copyright 2014 Hajar Farzaneh

ABSTRACT

This research investigates degradation of trichloroethylene (TCE) using a new treatment method called advanced reduction processes (ARPs). This new set of water treatment processes employ a source of activation energy to activate reducing agents and produce reducing radicals that can effectively degrade oxidized contaminants. Screening experiments were conducted to evaluate three different reducing reagents (sulfite, sulfide, and dithionite) and three UV light sources (low-pressure mercury UV lamp (UV-L), medium-pressure mercury UV lamp (UV-M), and narrow band mercury UV lamp (UV-N)) for TCE dechlorination in water. Both removal efficiency of TCE and chloride ion recovery were examined together to identify the best ARP. Results of screening experiments showed that ARP that combines UV-L with sulfite achieved the highest TCE removal efficiency and maximum chloride ion recovery.

Effects of experimental parameters on the kinetics and behavior of TCE dechlorination using sulfite/UV-L were investigated in order to obtain optimum operating conditions for TCE degradation. The experimental parameters that were evaluated are: TCE initial concentration, sulfite dose, solution pH, and light intensity. TCE photodegradation followed a first-order decay rate. Increasing pH value and increasing sulfite dose resulted in increasing TCE removal efficiency and almost complete degradation was achieved at pH 11 using 50:1 molar ratio of sulfite dose to initial TCE concentration with chloride ion being the major reaction product. TCE

dechlorination rate constant (k_{obs}) was independent of its initial concentration, whereas k_{obs} increased with increasing sulfite dose, pH, and light intensity.

DEDICATION

This thesis is dedicated to my parents for their love, endless support and encouragement.

ACKNOWLEDGEMENTS

I would like to thank my committee chair, Dr. Ahmed Abdel-Wahab, and my committee members, Dr. Mohamed Nounou and Dr. Eyad Masad for their guidance and support throughout the course of this research.

I would like to express my sincere and deepest appreciation to Dr. Bahngmi Jung for her patience, guidance and support over this research. She was a constant inspiration, and her assistance and suggestions were invaluable towards the completion of this research.

Special thanks go to Dr. Ahmed Khodary who was perfect guide in the lab work and gave me the reflection of good academic background on the practice of chemical engineering.

Also, I would like to thank my parents, who have always encouraged me to pursue my goals, always succeed, and never admit defeat.

Lastly, I sincerely thank all those who have directly or indirectly helped for the work reported herein.

NOMENCLATURE

e_{aq}^-	Hydrated electron
AOPs	Advanced oxidation processes
ARPs	Advanced reduction processes
ASRS	Anion self-regenerating suppressor
C	Concentration at time t
c	Speed of light= 3×10^8 m/s
C_0	Initial concentration
Conc.	Concentration
DCA	Dichloroethane
DCE	Dichloroethylene
DCP	Dichlorophenol
DDW	Deionized-deoxygenated water
ESR	Electron spin resonance
GC	Gas chromatogram
GC- μ ECD	Gas chromatogram equipped with micro-electron capture detector
GC-MS	Mass spectrometry gas chromatogram
h	Planck's constant= 6.626×10^{-34} J.s
$H\cdot$	Hydrogen radical
IC	Ion chromatogram
k_{obs}	Observed rate constant

MCL	Maximum contamination level
N_A	Avogadro's number= 6.022×10^{23} L/mol
NZLc	Nano-ZnO/Laponite composites
NZVI	Nanoscale zerovalent iron
OH•	Hydroxyl radical
PFOA	Perfluorooctanoic acid
PTFE	Polytetrafluoroethylene
R	Chloride ion recovery
Sol.	Solution
Std.	Standard
$t_{1/2}$	Half-life time
TCE	Trichloroethylene
USEPA	United States Environmental Protection Agency
UV	Ultraviolet
UV-L	Low pressure mercury vapor lamp
UV-M	Medium pressure mercury vapor lamp
UV-N	Narrowband mercury vapor lamp
VC	Vinyl chloride
VOA	Volatile organic analyte
VOC	Volatile organic compound
Vol.	Volume
λ	Light wavelength

TABLE OF CONTENTS

	Page
ABSTRACT	ii
DEDICATION	iv
ACKNOWLEDGEMENTS	v
NOMENCLATURE	vi
TABLE OF CONTENTS	viii
LIST OF FIGURES	x
LIST OF TABLES	xi
1. INTRODUCTION.....	1
2. LITERATURE REVIEW	7
2.1. TCE removal from water and wastewater	7
2.2. Advanced reduction processes	15
2.2.1. Ultraviolet light in ARPs.....	16
2.2.2. Reducing agents used in ARP	18
3. RESEARCH METHODOLOGY	22
3.1. Experimental methods.....	22
3.1.1. TCE stock and standard solutions	22
3.1.2. Samples preparation	23
3.1.3. Controlling solution pH.....	23
3.1.4. Chloride standards preparation.....	24

	Page
3.2. Activation method.....	26
3.3. Analytical methods.....	27
3.3.1. Gas Chromatography.....	27
3.3.2. Ion Chromatography	28
3.4. Precision and accuracy measurements	28
4. RESULTS AND DISCUSSIONS	31
4.1. Screening of different combinations of activating methods and reducing agents for TCE degradation.....	31
4.2. Characteristics of TCE degradation with UV-L/sulfite ARP.....	34
4.2.1. Effect of sulfite dose on kinetics of TCE degradation	37
4.2.2. Effects of initial TCE concentration	40
4.2.3. Effect of solution pH on TCE degradation kinetics	42
4.2.4. Effect of light intensity on Kinetics of TCE degradation	44
4.3. TCE degradation products.....	46
5. CONCLUSION	49
REFERENCES	51

LIST OF FIGURES

	Page
Figure 2.1: Proposed TCE reduction pathway	15
Figure 3.1: Experimental setup	26
Figure 4.1: Screening experiments for TCE removal efficiency with different reagents and UV light sources	33
Figure 4.2: Effect of sulfite dose on TCE degradation.....	39
Figure 4.3: Effect of initial TCE concentration.....	41
Figure 4.4: Effect of pH on TCE degradation	43
Figure 4.5: Effect of light intensity on TCE degradation.....	45
Figure 4.6: Chlorinated by-product peaks detected by GC-MS.....	48

LIST OF TABLES

	Page
Table 1.1: Physical and chemical properties of trichloroethylene	4
Table 1.2: Research plan summary	5
Table 2.1: Published data for TCE degradation products by UV photolysis	12
Table 3.1: TCE standard solutions	22
Table 3.2: Chemicals used and their specifications	25
Table 3.3: UV lights used in the research	26
Table 3.4: Accuracy measurements and calculations.....	29
Table 4.1: Screening test initial and final pH values.....	32
Table 4.2: Experimental conditions, calculated pseudo-first-order rate constants, and chloride recovery during TCE degradation by UV-L/Sulfite ARP.	36
Table 4.3: pH changes over time during the kinetic experiments.....	37

1. INTRODUCTION

Rapid industrial development and population increase led to increasing water demand worldwide. Furthermore, droughts and desertification which many countries are facing have resulted in increased concerns about water security and the need to maximize water reuse and recycle. Apart from the traditional water and wastewater treatment, new techniques for the production of usable water from industrial wastewater can provide large quantities of water that can be used for agriculture and other beneficial uses.

There are many industrial countries with very limited water resources, yet the demand on water is great due to industrial activities in these countries. Oil and gas industries produce large quantities of wastewater that can be utilized for agriculture and industrial activities. A number of techniques are available for the treatment of industrial wastewaters and the appropriate technique is chosen depending on the type of contaminants and the volumes of water to be treated. In many cases, conventional wastewater treatment technologies are ineffective for removals of persistent organic contaminants.

Advanced oxidation and reduction processes are attractive alternatives to traditional water and wastewater treatment which can destroy persistent contaminants. These processes utilize free radical reactions to directly destroy chemical contaminants. The formation of hydrogen radicals (H^{\bullet}) and the reducing hydrated electrons (e_{aq}^{-}) and/or

other reducing radicals (e.g. $\text{SO}_3^{\cdot-}$), can be effective in the removal of organic contaminants present in water and wastewater via chemical reduction.^{1,2}

A new technique that has been recently developed is advanced reduction processes (ARPs). This technology has been developed by combining activation methods and reducing agents to produce reactive reducing species which can destroy many oxidized contaminants.³ This process is similar to that utilized by advanced oxidation processes (AOPs). The difference between AOPs and ARPs is the production of reducing radicals in ARPs rather than oxidizing radicals (such as hydroxyl radicals) in AOPs.⁴ These ARPs have the tendency to efficiently destroy a wide range of oxidized contaminants such as chlorinated organics, perchlorate, nitrate, nitrite, chromate, arsenate, selenite, bromate and a number of radionuclides.⁵

Discharges of chlorinated solvents into subsurface environments have led to extensive soil and groundwater contamination. In addition, many industrial processes generate wastewaters contaminated with chlorinated solvent. The treatment of solutions containing chlorinated solvents has gained significant consideration in recent years.⁶ In this research the degradation of trichloroethylene, one of the chlorinated hydrocarbons, is investigated using advanced reduction processes.

Trichloroethylene (TCE) is a carcinogenic compound, nonflammable, colorless, and volatile organic compound (VOC) with a sweet odor comparable to ether or chloroform. It is considered as VOC because of its moderate boiling point and high vapor pressure. TCE is moderately water soluble and it is mainly used to remove grease from fabricated metal parts, as an extraction solvent for greases, oils, fats, waxes, and

tars. Also, it is used in some consumer products such as typewriter correction fluids, paint removers and strippers, adhesives, spot removers, and rug-cleaning fluids. TCE is not believed to occur naturally in the environment, but it has been found in some groundwater and many surface waters as a consequence of its production, inappropriate usage, and disposal. In United States most of the TCE released into the atmosphere is from industrial degreasing operations.⁷

Exposure to high levels of TCE can cause nervous system effects, liver and lung damage, irregular heartbeat, unconsciousness, and probably death. Digesting small quantities of TCE for long periods of time might cause liver and kidney damage, and weakened immune system function, although the extent of some of these consequences is not clear until this time.⁷

The maximum contaminant level (MCL) for TCE regulated by United States Environmental Protection Agency (USEPA) is 5 µg/L. MCLs are established to be as close to the health objectives as possible taking into consideration the cost, benefits, and the ability of public water systems to identify and eliminate contaminants using appropriate treatment technologies. USEPA also indicates regulations and standards for hazardous disposal in wastewater. According to these standards, TCE in disposed wastewater should not exceed 0.054 mg/L.⁸

Studies conducted on mice and rats have indicated that exposure to high levels of TCE may cause liver, kidney, or lung cancer. A number of studies on people exposed for long periods of time to high levels of TCE either in drinking water or in workplace atmosphere have found signs of increased cancer. Even though, there are some

uncertainties about the studies on people who were exposed to TCE, some of the effects found in people were similar to effects found in animals.⁷

TCE and other chlorinated organic compounds are the most dominant contaminants found in soil and groundwater that have serious health risks even at small concentrations. Wastewater from metal finishing, paint and ink production, electrical components, and rubber processing industries may contain TCE.⁹

Physical and chemical properties of TCE are presented in Table 1.1.

Table 1.1: Physical and chemical properties of trichloroethylene⁷

Property	Information
Chemical Formula	C_2HCl_3
Chemical Structure	$ \begin{array}{c} \text{H} \quad \quad \text{Cl} \\ \backslash \quad / \\ \text{C} = \text{C} \\ / \quad \backslash \\ \text{Cl} \quad \quad \text{Cl} \end{array} $
Molecular Weight	131.40
Color	Clear, colorless
Physical State	Liquid (at room temperature)
Melting Point	-87.1°C
Boiling Point	86.7°C
Density	1.465 g/mL (at 20°C)
Odor	Ethereal; chloroform-like; sweet
Solubility	1.070 g/L (water at 20°C) 1.366 g/L (at 25°C)
Organic Solvents	Miscible with many common organic solvents (such as ether, alcohol, and chloroform)
Vapor Pressure	74 mmHg (at 25°C)

The main goal of this research is to evaluate the effectiveness of ARPs for destroying TCE in water. In order to achieve this goal, four main tasks were conducted. The first task (Task 1) was to develop experimental and analytical procedures, the second task (Task 2) was to screen different combinations of activating methods and reducing agents and identify the optimum combination that achieve the maximum TCE degradation efficiency. The third task (Task 3) was to characterize TCE degradation kinetics using the optimum ARP condition identified by Task 2 and to evaluate effects of operating parameters on the behavior of TCE degradation. The fourth task (Task 4) was to understand reaction mechanisms and develop kinetic model for TCE degradation.

Table 1.2 summarizes the tasks and corresponding methodologies required to meet the research objectives.

Table 1.2: Research plan summary

Task	Methodology	Expected Benefit
Task 1: Develop experimental and analytical method	<ul style="list-style-type: none"> • Develop the reactor system and batch experimental procedures • Solvent extraction for TCE analysis using GC-μECD • Ion chromatography for chloride 	<ul style="list-style-type: none"> • Reliable experimental procedures and reproducible analytical methods

Table 1.2: Continued

Task	Methodology	Expected Benefit
<p>Task 2: Screen different combinations of activation methods and reducing agents</p>	<ul style="list-style-type: none"> • Experiments with different reducing agents and UV light sources • Reducing agents: sulfite, dithionite, sulfide • UV light sources: UV-L, UV-M, UV-N 	<ul style="list-style-type: none"> • Ability to identify the optimum combination that achieve maximum TCE degradation efficiency
<p>Task 3: Characterize TCE degradation kinetics for the optimum ARP combination identified by Task 2</p>	<ul style="list-style-type: none"> • Batch kinetic experiments with varying solution pH, sulfite dose, TCE initial concentration, and UV light intensity • Measured variables: TCE concentration, pH, chloride concentration 	<ul style="list-style-type: none"> • Ability to evaluate extent and rate of TCE degradation as affected by important process variables
<p>Task 4: Understand reaction mechanism for TCE removal by ARP and develop the kinetic model for TCE degradation</p>	<ul style="list-style-type: none"> • Nonlinear regression computation for obtaining the appropriate kinetic model parameters. 	<ul style="list-style-type: none"> • Ability to evaluate the rate of degradation and kinetic parameters.

2. LITERATURE REVIEW

2.1. TCE removal from water and wastewater

Many TCE removal processes have been reported. These treatment processes include bioremediation, thermal treatment, chemical oxidation, and electro-kinetic remediation.^{9, 10} Conventional treatment technologies such as air stripping and adsorption on activated carbon are effective in removing TCE from polluted waters, but in these cases TCE is transferred from one phase to another without being destroyed.¹¹⁻¹³ Previous studies for removal of TCE from soil, groundwater and wastewater, focused mainly on bioremediation techniques¹¹, as well as some extensive research on the photo-induced and AOPs as an alternative environmental degradation methods to degrade TCE efficiently.¹²⁻¹⁴

TCE photolysis was widely studied in liquid and gaseous phase as direct photolysis with ultraviolet (UV) irradiation. Some researchers attempted to enhance the photolysis of TCE using different catalysts. TiO₂ was commonly used in many studies with effective degradation.¹⁵⁻²⁴ Adhikari et al. investigated the removal of TCE from drinking water by both photolysis and sonolysis. They used UV light source with a wavelength of 254 nm to study the photolysis of TCE solution containing TiO₂. A cup-horn, flow-through reactor system was used and 84% TCE removal was achieved by UV light irradiation while only 25% removal was obtained with ultrasound.²³ Rather than the combination of TiO₂ and UV light, some researchers observed efficient TCE degradation using UV/H₂O₂.^{12, 25-27} Dobaradaran et al. studied the degradation of TCE at micromolar

concentrations by UV/H₂O₂.^{12, 27} Different initial pH values (pH 3, 5, 7, and 11) were tested but TCE degradation rate was not affected by initial pH. They observed an increase in the degradation rate with decreasing the initial concentration of TCE (the rate constant was 0.0348 min⁻¹ when TCE initial concentration was 380.5 μM and it became 0.1766 min⁻¹ when the initial concentration decreased by 100 times to 3.8 μM). Dobaradaran et al. also reported an increase in TCE degradation by increasing molar ratio of H₂O₂ to TCE initial concentration. Based on their studies no harmful byproducts were detected at low initial TCE concentrations (0.22, 2.28, and 22.83 μM) and chloride was the major end product with 95.5% degradation efficiency after 70 min reaction time. When they increased the initial concentration of TCE to 380 μM, they found formic acid, dichloroacetic acid, dichloroacetylene, formaldehyde, and glyoxylic acid whereas dichloroacetylene and formaldehyde were completely removed after 70 min degradation time. A study by Weir et al. on TCE oxidation by UV/H₂O₂ reported similar results with first-order rate which depends on TCE initial concentrations and light intensity.²⁵ Weir et al. had found that increasing H₂O₂ to a certain amount followed first order degradation rate but it became independent of peroxide concentration after reaching a maximum at high peroxide levels. Wang et al. tried to compare TCE advanced oxidation by UV/H₂O₂ and UV/chlorine with direct photolysis at different pH values with medium pressure mercury UV lamp.²⁶ They observed more efficient degradation by UV/H₂O₂ at neutral and alkaline pH while at pH 5 UV/chlorine showed better removal. Wang et al. explained these results by the formation of different scavengers of OH• at different pH values and OCl⁻ formation at alkaline pH. The rate of degradation by direct photolysis

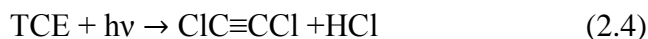
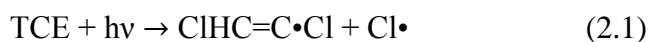
was found to be slower than AOPs since TCE in AOP is rapidly oxidized by OH•. A recent study by Dobaradaran et al. compared the TCE removal efficiency by direct photolysis and UV/H₂O₂ AOP and found complete TCE removal at very low initial TCE concentrations (3.8 and 7.6 μM) by both direct photolysis and UV/H₂O₂.²⁷ According to their study, TCE was completely removed by UV/H₂O₂ with increasing the initial TCE concentration to higher values (76.1 and 190.3 μM), but the removal efficiency decreased to 91% and 88.4% at 76.1 and 190.3 μM initial TCE concentration, respectively by direct photolysis.

Parshetti and Doong were able to dechlorinate TCE effectively under anoxic conditions by Fe/TiO₂ nanocomposites in presence of nickel ions and UV light at 365 nm.^{28, 29} They found that the degradation of TCE was significantly enhanced by increasing the amount of nickel ions whereas increasing pH decreased the rate of dechlorination. They also tried to degrade TCE by nanoscale zerovalent iron (NZVI) but they observed slower degradation comparing to the Fe/TiO₂ nanocomposite. In addition, they studied the dechlorination of TCE in the dark and they reported 20%, 66%, and 87% TCE removals using TiO₂, NZVI, and Fe/TiO₂, respectively in 145 hours. UV illumination at 365 nm for 100 min did not achieve significant degradation by direct photolysis and little removal was observed in the presence of TiO₂ and Fe/TiO₂.²⁸ Joo et al. used nano-ZnO/Laponite composites (NZLc) as an alternative photocatalysts to degrade TCE which can reduce the difficulties of filtration and photocatalysts recovery.³⁰ Based on their investigation, TCE was removed by NZLc under UV irradiation by sorption, photolysis, and photocatalysis. According to their results, the

degradation rate decreased by increasing TCE initial concentration whereas, it was increased by increasing the amount of NZLc to a certain value and the rate did not increase further due to the block of UV radiant flux. In addition, they observed faster degradation by increasing pH (greater than 7).

A study by Chu and Jia on TCE photodegradation using three different monochromatic UV lamps (254, 300, and 350 nm) showed the highest TCE removal rate by the 254 nm UV lamp.³¹ They found the maximum absorption wavelength of TCE at 213 nm which is near to UV lamp emitting light at 254 nm. According to their observations TCE degradation rate was decreased as the wavelength of the UV light was increased. The degradation rates followed the pseudo first-order decay kinetics in all cases and the rate of degradation was found to decrease by increasing the initial TCE concentration.

TCE can be degraded in both oxidative and reductive pathways. In oxidative pathway, TCE is degraded by the formation of oxidative agents such as hydroxyl radical. TCE degradation by oxidation methods usually results in the formation of toxic intermediates such as formaldehyde, dichloroacetylene, etc. Li et al. extensively studied TCE oxidation by direct photolysis and they had proposed the following reactions to be the major reaction pathways for TCE decay.¹³





Equation 2.1 shows the homolytic cleavage of C-Cl bond, generating a carbon-centered radical and chlorine radical. Equations 2.3 and 2.4, which were proposed by Mertens and Sonntag, shows UV photolysis of TCE.³² In Equation 2.3, TCE loses molecular chlorine and produces monochloroacetylene. In Equation 2.4, TCE loses HCl and produces dichloroacetylene. Equation 2.2 shows TCE photolysis producing a precursor of dichloroacetaldehyde ($\text{Cl}_2\text{HC-CHO}$). The chlorine radicals can be generated through the photolysis of TCE or other chlorinated species. Chlorine radical is known to be a strong electrophile, and that it can remove the double bond of TCE ($\text{Cl}_2\text{HC-C}\cdot\text{Cl}_2$) as shown in Equation 2.5.

Recently, TCE degradation by reductive methods gained more interest. In reductive pathway, reducing agents are used to dechlorinate TCE by replacing chlorine in TCE with hydrogen ions. In this manner, Parshetti and Doong proposed hydrodechlorination to be the major reaction pathway for TCE dechlorination by Fe/TiO₂ nanocomposites under anoxic conditions in the presence of nickel ions and UV light at 365 nm. They found that 90-94% of ethane was recovered from TCE dechlorination by Fe/TiO₂ under dark conditions according to reaction shown in Equation 2.6, whereas TCE was not dechlorinated at all after 120 min of UV illumination when it is copresent with 2,4-dichlorophenol (DCP).²⁸



Table 2.1 shows some of the published data for TCE degradation products by UV photolysis.

Table 2.1: Published data for TCE degradation products by UV photolysis

Reductant/Catalyst	Phase	Major degradation products	Minor degradation products	Removal efficiency	Ref.
H ₂ O ₂	aqueous	Chloride ion	Formic acid, dichloroacetic acid, glyoxylic acid, oxalic acid	95.5%	12
TiO ₂ in fluorocarbon solvent	aqueous	Dichloroacetic acid	Chloride ion	40%	15
TiO ₂	gaseous	Dichloroacetylene chloride, phosgene		83%	18
Sol-gel TiO ₂ /Cr, Fe, Ni, Cu, Pt, Ca(OH) ₂	gaseous	COCl ₂ , CHCl ₃ , CHCl ₂ COCl	Chloride ion, CHCl ₂ COO ⁻ , CO ² (no chlorinated products detected with Cu and Ca(OH) ₂)	26-30% mineralized to CO ₂	19
TiO ₂	gaseous	CO ₂ , HCl, Cl ₂ , COCl ₂ , ClCOCOCl, CHCl ₃ , CHCl ₂ COCl, CHCl ₂ CH ₂ Cl		99.9%	20
TiO ₂ glass fiber cloth	gaseous	Phosgene, 1,1-DCE, oxalyl chloride, ethane pentachloride, CO ₂	Dichloroacetylene chloride, dichloroacetic acid	~70%	21

Table 2.1: Continued

Reductant/Catalyst	Phase	Major degradation products	Minor degradation products	Removal efficiency	Ref.
TiO ₂ , O ₃	gaseous	CO ₂ , Chloride ion	Non-identified chlorinated and organic intermediates	97%	22
TiO ₂ films	gaseous	Dichloroacetylene chloride		60-100%	24
H ₂ O ₂	aqueous	Chloride ion, dichloroacetic acid, glyoxylic acid	Formic acid, dichloroacetaldehyde, chloroform, formaldehyde, oxalic acid	95.8-100%	27
Titania/silica	gaseous	Phosgene	Chloroform, carbon tetrachloride	88%	33
Fe/TiO ₂ nanocomposites	aqueous	Ethane		90%	29

Gantzer and Wackett had proposed that the reduction of chlorinated ethenes occur via sequential hydrogenolysis.³⁴ According to their report, TCE can go through a sequence of hydrogenolysis process and produce cis-/trans-/1,1-dichloroethylene (DCE), vinyl chloride (VC), and ethene when catalyzed by bacterial transition metal coenzymes. Hydrogenolysis is simply the breaking of a chemical bond in an organic molecule with the simultaneous addition of a hydrogen atom. In addition to the hydrogenolysis, Burris et al. have proposed the reductive β -elimination as a significant reaction pathway after observing acetylene as a reactive intermediate and the formation of a trace amount of chloroacetylene in reductive dechlorination by vitamin B₁₂ in homogeneous and heterogeneous systems.^{6, 35} Reductive β -elimination is a reaction in which functional group is removed from one carbon and other group is removed from the other carbon. In β -elimination there is loss of two single bonds and formation of one triple bond. Reductive β -elimination of TCE would yield chloroacetylene while reductive β -elimination of either cis- or trans-DCE yields acetylene. They also suggested that 1,1-DCE can lose its two chlorine atoms which are bonded to the same carbon of the molecule to form ethene by reductive α -elimination. Figure 2.1 illustrates TCE reduction pathway as proposed by Burris et al.

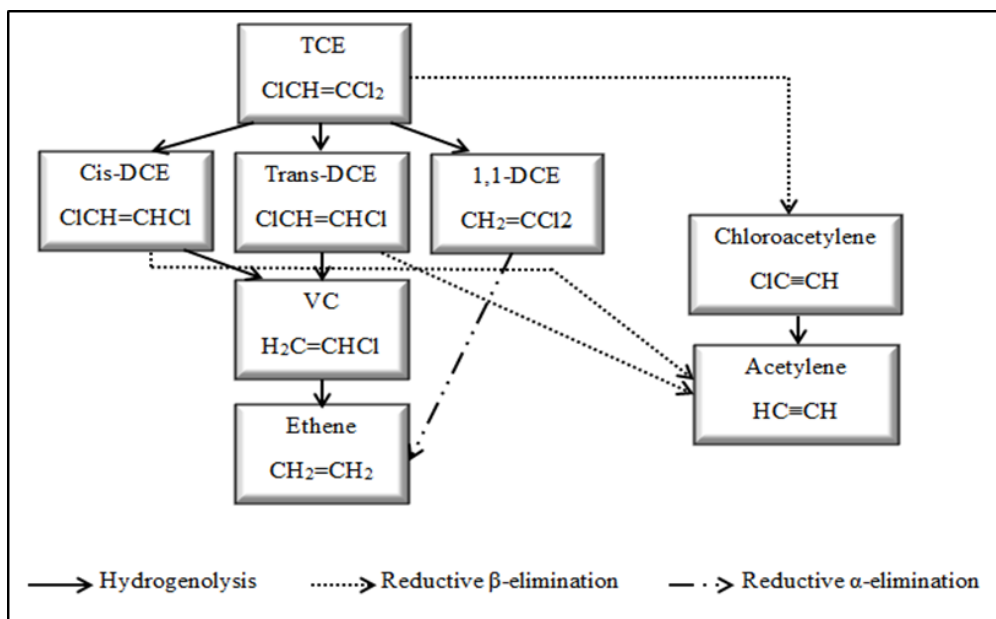


Figure 2.1: Proposed TCE reduction pathway

2.2. Advanced reduction processes

Recently, there has been interest in chemical degradation using advanced reduction processes (ARPs).^{3-5, 36-41} In ARPs a reducing agent is combined with an activating method to produce highly reactive reducing radicals. As these free radicals are species with an unpaired electron, they can either donate their unpaired electron and acting as effective reductants or they can accept an electron and form a pair of electron and act as effective oxidants. In treatment processes, the kinetics of these redox reactions is the critical factor to determine the effectiveness of degrading the target compound. These highly reactive reducing radicals make the kinetics of desired reactions viable while they might be very slow with common reductants.⁴

In ARP different activation methods and reducing agents can be used to effectively degrade compounds depending on their chemical and physical properties. Some possible activation methods which are used are: ultraviolet light, ultrasound, electron beam, and microwave. Reducing agents which are used in ARPs include dithionite, sulfite, sulfide, and ferrous iron. In this research UV lights with different wavelength outputs are used to activate sulfite, dithionite, and sulfide to degrade TCE. The combination showing the most efficient TCE removal was used to investigate the effect of process variables on TCE dechlorination kinetics.

2.2.1. Ultraviolet light in ARPs

UV light with different wavelength outputs was used in ARPs and the desired wavelength depends on the absorption spectra of the reagent to be activated. Low pressure mercury vapor lamp (UV-L) is currently used in water and wastewater treatment with a wavelength of 254 nm. UV-L produces 33-40% of UV-C, which is a band of the short-wave ultraviolet radiation in the range of 100-280 nm which is lethal to microorganism and mostly used for disinfection of drinking water and wastewater. Higher energy can be provided by photons at shorter wavelength so they have enough energy to break chemical bonds and produce free radicals.⁴⁰ In addition to UV-L lamps, medium pressure mercury vapor lamp (UV-M) is also used in some degradation and disinfection processes. UV-M lamps emit light at a wavelength between 200-600 nm with majority of their UV output in the UV-A and UV-B spectral areas (UV-M lamps emit maximum 7-10% of UV-C spectrum).⁴² UV-A has a long-wave UV radiation in the

range of 315-400 nm and it is also known as the black light, while UV-B range is for the medium-wave UV radiation (280-315 nm). UV-L lamps are more preferable than UV-M since they are more cost efficient due to low energy consumption and they have longer life and produce less heat comparing to UV-M lamps.⁴² Another type of UV lamp is the narrowband lamp (UV-N), which mainly emits light ranged from 280 nm to 320 nm with peak irradiance at 312 nm. Vellanki et al. reported that UV-N may be more efficient to produce free radicals from dithionite because dithionite absorb light at wavelength 315 nm.⁴ UV-L was found to be the most effective activation method in ARP and it was successful for degradation of vinyl chloride (VC)^{3, 43}, 1,2-dichloroethane (1,2-DCA)^{36, 37, 43}, perfluorooctanoic acid (PFOA)^{4, 44}, perchlorate^{4, 39}, nitrate^{38, 4}, and dichlorophenol (DCP).⁴ Yoon et al. attempted to study the degradation of 1,2-DCA by UV-N and UV-M.³⁶ They found that 1,2-DCA was degraded effectively with UV-M combined with sulfite, sulfide, or dithionite, whereas with UV-N the degradation was slower and the efficiency of ARP was dependent on the solution pH (better removal at high pH). Vellanki et al. have conducted a screening test for different target compounds (nitrate, perchlorate, DCP, and PFOA) by both UV-L and UV-N and they reported good removal of DCP and nitrate by UV-L, while UV-N could only degrade DCP with sulfide, sulfite and ferrous iron.⁴ Bensalah et al. reported that nitrate can be better degraded by UV-M comparing to UV-L and UV-N.³⁸ UV-M was also used by Bensalah et al. for bromate degradation.⁴¹

2.2.2. Reducing agents used in ARP

Different reducing agents can behave differently when irradiated with UV Light depending on the UV light sources because different agents absorb light at different wavelengths. Dithionite, sulfite, and sulfide have been generally used in previous ARP studies and their behaviors are briefly described in this section.

Dithionite

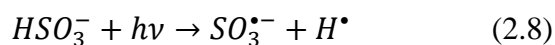
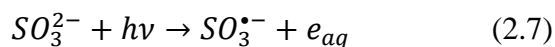
Dithionite ($S_2O_4^{2-}$) has a weak S-S bond that can easily break and form two sulfur dioxide radicals ($S_2O_4^{2-} + h\nu \rightarrow 2SO_2^{\bullet}$) which are known to be strong reductants.^{45,46} Both dithionite and sulfur dioxide radicals are strong reductants. It has been reported that the standard reduction potential of sulfur dioxide radical is -0.66V (at pH 7 and 25°C)⁴⁵ and dithionite has a reduction potential of -1.12V in strongly basic solutions.⁴⁶ Dithionite can be activated by different methods to increase the production of sulfur dioxide radical. The light absorption peak of dithionite is at 315 nm wavelength.⁴ Dithionite activation by UV light was realized after observing the production of hydrogen when dithionite was irradiated with a high pressure mercury lamp.⁴⁷

Yoon et al. have demonstrated that unpaired electrons from sulfur dioxide radical formed by UV irradiation can be transferred to the electron acceptor, 1,2-DCA, resulting in 1,2-DCA degradation ($DCA + SO_2^{\bullet} \rightarrow \text{products}^{\bullet} + SO_2$).³⁶ Liu et al. reported that dithionite irradiation by UV-L led to a complete 1,2-DCA degradation in 120 min.³⁷ Yoon et al. have found that dithionite activated by UV-M and UV-N irradiation resulted in a complete 1,2-DCA degradation in few minutes under basic pH condition.³⁶ At

neutral pH, dithionite/UV-N ARP showed slower 1,2-DCA but 1,2-DCA was completely degraded in 2 hours.³⁶ Regardless of UV lamp source, dithionite showed a complete and fast 1,2-DCA degradation. Yoon et al. described a slow 1,2-DCA degradation rate at low pH by the formation of intermediate products other than $SO_2^{\bullet-}$ formed from dithionite decomposition reactions at low pH such as bisulfite.³⁶ However, the free radicals from intermediate products including bisulfite also may be potential reductants at acidic pH. In an ARP study on vinyl chloride degradation by dithionite/UV-L, Liu et al. found better degradation at higher pH indicating that dithionite can absorb more light at higher pH.⁴⁰ According to Vellanki et al. study on dithionite/UV-L ARP of different contaminants, they reported good removal of nitrate, moderate removal of DCP, low removal of PFOA, and negligible removal of perchlorate. On the other hand, with dithionite/UV-N combination low removal of PFOA and negligible removal of the other three compounds (DCP, nitrate, and perchlorate) were obtained after 20 hours irradiation time.⁴ Bensalah et al. reported that dithionite/UV-M can degrade nitrate more efficiently than UV-L and UV-N. They also reported better nitrate removal at alkaline and neutral pH, while nitrate degradation at acidic pH was found to be negligible.³⁸

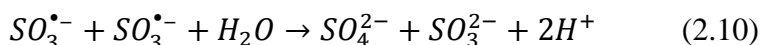
Sulfite

Both hydrated electron (e_{aq}) and sulfite radical anion ($SO_3^{\bullet-}$) can be formed from sulfite irradiated with UV, as shown in Equation 2.7. It may also produce hydrogen radical (H^{\bullet}) when HSO_3^- is predominant at low pH, as shown in Equation 2.8.³⁶



UV absorption peak of sulfite solutions depends on pH. Reaction shown in Equation 2.7 is preferred at neutral and basic pH conditions, while reaction shown in Equation 2.8 is dominant at acidic pH.

The hydrated electron is a strong reductant with a standard reduction potential of about -2.9 V, and it is used for degradation and detoxication of halogenated organic compounds.^{48, 49} Hydrogen atom (H^\bullet) is an active reducing agent with standard reduction potential of -2.3 V,⁴⁸ whereas sulfite radical anion ($SO_3^{\bullet-}$) acts as both oxidizing and reducing reagent. Equation 2.9 shows that sulfite radical can react with aqueous electron to produce sulfite ion. Also sulfite radicals can recombine to form sulfate and sulfite as shown in Equation 2.10.^{50, 51}

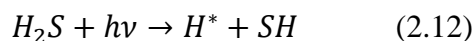
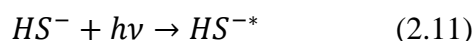


Liu et al. investigated the effects of several experimental factors on the degradation rate of vinyl chloride by sulfite/UV-L ARP. They observed the largest rate constant at pH 9 while complete dechlorination was achieved at other pH values investigated but with slower rate.³ Song et al. found a complete degradation of perfluorooctanoic acid by sulfite/UV-L after one hour of irradiation. Also, they found that PFOA degradation rate was accelerated by increasing either sulfite dose or solution pH.⁴⁴ In another study on nitrate, Vellanki and Batchelor observed increasing degradation rate by increasing pH and temperature. This study showed that nitrate reduction rate increased with increasing sulfite dose up to a certain limit after which additional sulfite dose did not affect rate of nitrate reduction.³⁹ Liu et al. achieved more

than 90% degradation of initial 1,2-DCA concentration by sulfite/UV-L within 20 min in alkaline conditions, while the same removal percentage was achieved after 130 min at pH 7.³⁷ Yoon et al. reported complete 1,2-DCA removal by both UV-M and UV-N but with slower degradation rate at acidic conditions.³⁶

Sulfide

Sulfide absorbs UV light at 230 nm wavelength and produces reactive species such as bisulfide radical (HS^{-*})⁵² or hydrogen (H^*)⁵³ when irradiated to UV light as follows:



Liu et al. obtained high degradation efficiency of VC by sulfide/UV-L ARP at pH 7. They proposed that the dominant species of sulfide at pH 3 would be H_2S and at pH 10 it would be HS^- while at neutral pH both H_2S and HS^- would have equal concentrations.⁴⁰ A similar ARP study on 1,2-DCA degradation by sulfide/UV-L reported good removal at high pH and negligible removal at acidic conditions.³⁷ Whereas Yoon et al. reported higher degradation of 1,2-DCA at acidic condition by sulfide/UV-M comparing to that at neutral pH.³⁶ Vellanki et al. found that nitrate and 2,4-dichlorophenol (2,4-DCP) can be effectively removed by sulfide/UV-L.⁴

3. RESEARCH METHODOLOGY

3.1. Experimental methods

All solutions were prepared in an anaerobic chamber (Coy laboratory products) filled with nitrogen gas. All the aqueous solutions were prepared using deionized-deoxygenated water (DDW). DDW was prepared by purging high purity nitrogen gas (99.9995%) into deionized water for at least 2 hours.

3.1.1. TCE stock and standard solutions

A stock solution of 5050 ppm TCE in 40 mL methanol was prepared daily to prevent TCE loss. The standard solutions were prepared fresh in order to get a new standard calibration curve whenever TCE is analyzed. Standard solutions were prepared in 40 mL hexane with the concentrations listed in Table 3.1.

Table 3.1: TCE standard solutions

Std.	Vol. from Stock Sol. (μL)	Conc. (mg/L) ppm	Conc. (mM)
1	8	1.0098	0.0077
2	40	5.0449	0.0384
3	80	10.0798	0.0767
4	160	20.1195	0.1531
5	240	30.1193	0.2292
6	320	40.0794	0.3805

The reactor containing both stock and standard solutions was 40-mL volatile organic analyte (VOA) vials screw top with PTFE/silicon septa caps. The required volume of TCE was injected into the vials using Hamilton gas-tight syringes through the septum of the cap after filling the vials with 40 mL of either methanol or hexane.

3.1.2. Samples preparation

42 mL quartz reactor crimp top cells (purchased from J&J Science, South Korea) with butyl rubber septa and aluminum caps were used for the batch kinetic experiments. The quartz cells were filled with 40 mL of pH-controlled sulfite solution and the cap was closed. Then, the required volume from the stock solution was injected into the quartz cells using gas-tight syringe to obtain the required initial concentration of TCE in each sample. The prepared samples were shaken for 30 minutes with 250 rpm (VWR model 3500 orbital shaker) and taken to the UV chamber with the specified light intensity. At the desired sampling time, 4 mL of the solution is removed from the quartz cells with a gas-tight syringe and transferred to 20 mL amber screw capped vials containing 4 mL hexane to extract TCE from the sample. This solution is shaken vigorously using vortex mixer for 20 seconds. Then, 2 mL supernatant is taken from the extraction vial and transferred to 2-mL vials for GC analysis.

3.1.3. Controlling solution pH

To control solution pH at the desired value, 0.1 M phosphate buffer was prepared at pH 7 then appropriate volume of 1 N NaOH (for basic conditions) or 1 N HCl (for

acidic conditions) was added to adjust the solution pH to the desired value for the kinetic experiments. To prepare 0.1 M of pH 7 phosphate buffer solution, the following procedure was followed in anaerobic conditions:

1. Preparing 0.2 M monobasic sodium phosphate: 27.6 grams of monobasic sodium phosphate is dissolved with DDW to make 1 liter solution.
2. Preparing 0.2 M dibasic sodium phosphate: 28.4 grams of dibasic sodium phosphate is dissolved with DDW to make 1 liter solution.
3. 39 mL of 0.2 M monobasic sodium phosphate (step 1) is mixed with 61 mL of dibasic sodium phosphate (step 2).
4. 100 mL of DDW is added to the prepared solution (step 3) to make 0.1 M phosphate buffer with pH 7.
5. pH is measured to insure the accuracy of the solution pH.

For the kinetic experiments, a total concentration of 5 mM of buffer solution was used by diluting the prepared 0.1 M phosphate buffer.

3.1.4. Chloride standards preparation

Chloride ion recovery was measured to quantify the concentration of TCE that was reduced completely. Chloride ion concentration was measured to calculate its recovery as it is removed while TCE is degraded. The total amount of chlorine existed in the specified initial TCE concentration is calculated by the stoichiometric ratio knowing that there are 3 moles of chlorine in 1 mole of TCE (C_2HCl_3). To analyze chloride ion, sodium chloride was used to prepare standard chloride solution.

A stock solution of 1000 ppm of chloride was prepared by dissolving 1.648 grams of NaCl in DDW to make 1 L NaCl solution. This stock solution was used to prepare 5, 10, 20, 30, and 40 ppm standard solutions for ion chromatography calibration.

Table 3.2 shows the specifications of chemicals used in this research and Figure 3.1 illustrates the experimental setup.

Table 3.2: Chemicals used and their specifications

Chemical name	Chemical formula	Vendor	Specifications
Trichloroethylene	C_2HCl_3	Sigma-Aldrich	ACS reagent, $\geq 99.5\%$
Methanol	CH_3OH	Sigma-Aldrich	$\geq 99.9\%$, A.C.S. spectrophotometric grade
Hexane	C_6H_{14}	Sigma-Aldrich	Anhydrous, 95%
Sodium sulfite	Na_2SO_3	Fisher Scientific	Anhydrous, analytical reagent grade
Monobasic sodium phosphate	NaH_2PO_4	Sigma-Aldrich	ACS reagent 98-102%
Dibasic sodium phosphate	Na_2HPO_4	Mallinckrodt Chemicals	USP-GenAR
Sodium chloride	$NaCl$	Fisher Scientific	Analytical reagent grade, conforms to EP and ACS
Sodium hydrosulfite (sodium dithionite)	$Na_2S_2O_4$	Sigma-Aldrich	$\geq 82\%$ RT
Sodium sulfide	Na_2S	Fisher Scientific	Anhydrous, analytical reagent grade

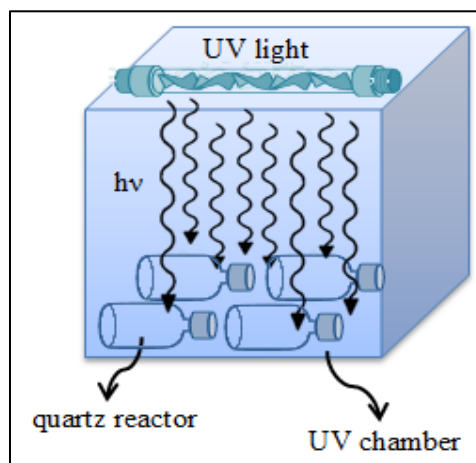


Figure 3.1: Experimental setup

3.2. Activation method

UV light from a UV irradiation chamber obtained from BioLink, Vilber Lourmat, was used as the activating method in this research. The chamber has dimensions of 14.5 cm height, 33 cm depth, and 26 cm width. Three different types of UV lamps were used, low mercury pressure (UV-L), medium pressure (UV-M), and narrow band (UV-N). The specifications of these lamps are illustrated in Table 3.3.

Table 3.3: UV lights used in the research

UV type	Lamp	Manufacturer	Wavelength
UV-L	T-8C (8W)	Vilber Lourmat, France	Monochromatic at 254 nm
UV-M	T-8L (8W)	Vilber Lourmat, France	320 – 380 nm with peak irradiance at 365 nm
UV-N	T-8M (8W)	Vilber Lourmat, France	280 – 320 nm with peak irradiance at 312 nm

3.3. Analytical methods

To analyze TCE concentration in the samples, gas chromatogram was used, while chloride ion concentration was analyzed by ion chromatography. The analytical procedures used for these two analytes are described in the following subsections.

3.3.1. Gas Chromatography

TCE concentration was analyzed using Agilent Technologies 7890A gas chromatography (GC) system equipped with micro-electron capture detector (μ ECD) with the following conditions:

- Carrier: Helium, total flow 44.929 mL/min with a makeup N₂ flow of 20 mL/min
- Column: Agilent Technologies J&W 123-1035 (DB-1), 30 m \times 320 μ m \times 5 μ m
- Injection: Split mode with a ratio of 10:1 and a volume of 0.1 μ L at 210°C
- Oven temperature:
 - Start at 40°C and hold for 3 minutes
 - Ramp of 10°C/min to 150°C and hold for 2 minutes
 - Ramp of 20°C/min to 180°C and hold for 1 minute
- Detector temperature: 280°C

The degradation by-products were analyzed by mass spectrometry GC (Varian GC-MS) with similar column and oven program indicated above.

3.3.2. *Ion Chromatography*

To analyze the concentration of chloride, Dionex ICS-5000 ion chromatogram (IC) was used. This IC system is equipped with dual gradient pump, AS autosampler, and eluent generation module with the following conditions:

- Eluent: 4.5 mM Na₂CO₃ / 0.8 mM NaHCO₃
- Flow rate: 0.25 mL/min
- Temperature: 30°C
- Detection: Suppressed conductivity
- Suppressor: Anion self-regenerating suppressor (ASRS 300, 2mm)
- Applied current: 7 mA
- Injection volume: 1200 µL

3.4. **Precision and accuracy measurements**

As an initial step, the precision and accuracy tests for TCE were conducted. To evaluate the accuracy and precision, 6 TCE solutions were prepared with the same concentration of 1.0098 ppm (0.0077 mM) and analyzed with GC-µECD.

Accuracy, which refers to the closeness of a measured value to a standard or known value, was calculated for all the 6 samples by calculating the recovery for each of the prepared samples and taking the average. The percentage of recovery can be calculated by dividing the measured TCE concentration by the desired concentration. The results of these calculations are indicated in Table 3.4.

Table 3.4: Accuracy measurements and calculations

Sample No.	Measured TCE Conc. (ppm)	Recovery (%)
1	0.8582	84.99
2	1.0333	102.33
3	1.0136	100.38
4	1.0664	105.61
5	1.1000	108.93
6	1.0654	105.51
Average	1.0228	101.29% (Accuracy)

Precision, which refers to the closeness of two or more measurements to each other, was found by calculating the relative standard deviation as follows:

$$\begin{aligned} \text{Relative standard deviation} &= \frac{\text{Standard deviation}}{\text{average}} \times 100 = \frac{0.086}{1.0228} \times 100 \\ &= 8.4\% \text{ (Precision)} \end{aligned}$$

In addition to the accuracy and precision, the detection limit of GC- μ ECD was calculated by multiplying the standard deviation by the student t-value at a confidence level of 99%. According to the student's t-distribution for a degree of freedom of 5 with a 99% confidence, the student t-value is 3.365.

Using the calculated standard deviation and the related student t-value, the detection limit can be calculated as follows:

$$\text{Detection limit} = (\text{standard deviation}) \times (\text{student t-value}) = 0.289 \text{ ppm} = 0.00219 \text{ mM}$$

The results obtained from the precision and accuracy calculations indicate that both the preparation method and the analytical procedure are reliable to conduct accurate and precise experiments. The detection limit gives an approximated minimum value of TCE concentration that can be measured by GC- μ ECD.

4. RESULTS AND DISCUSSIONS

4.1. Screening of different combinations of activating methods and reducing agents for TCE degradation

Screening experiments were conducted with each combination of three different reducing agents (sulfite, sulfide, and dithionite) and three UV light sources (UV-L, UV-M, and UV-N) resulting in nine experiments. The irradiation time for these experiments was fixed at 3 hours. These experiments were conducted without controlling solution pH but initial and final pH values were measured and are illustrated in Table 4.1. The pH increase was found to be for UV-L/sulfite which indicates the consumption of hydrogen ions in the reactions which can replace chloride to produce non-chlorinated compounds.

Figure 4.1 shows results of screening experiments and indicates that UV-L, monochromatic at 254 nm generally showed a high TCE removal above 90%, regardless of the types of reducing agent. Also UV-L alone without a reducing agent showed TCE removal approaching 90% while it was neither removed by UV-M nor by UV-N without reducing agents. The decrease in the pH value with UV-L without reducing agent indicates the release of protons mainly from TCE photolysis. This result agrees with Chu and Jia observation as they found decrease in pH (from 4 to 2.8) in 20 min when they investigated the decay of TCE with direct photolysis using 254 nm monochromatic UV lamp.³¹ They also investigated monochromatic UV lamps with 300 nm and 350 nm and they found lower degradation rate comparing to the 254 nm lamp. Whereas Parshetti and

Doong observed insignificant TCE removal when they used UV irradiation at 365 nm in anoxic conditions.²⁸

The highest TCE removal of 97.6% was obtained with UV-L/sulfite ARP. Also, the combinations of UV-N or UV-L with sulfide achieved relatively high TCE removal of more than 85% but slightly less than the removal efficiency obtained with UV-L/sulfite. UV-M was not efficient with any of the three reducing agents showing less than 25% of TCE removal in all cases. Dithionite irradiated by UV-N achieved little removal, less than 20%.

Table 4.1: Screening test initial and final pH values

		No reducing agent	Sulfite	Sulfide	Dithionite
Initial pH		4.49	8.35	11.93	3.27
Final pH	UV-L	3.41	11.19	12.23	2.91
	UV-M	5.45	8.60	11.85	2.83
	UV-N	4.14	8.59	11.76	2.79

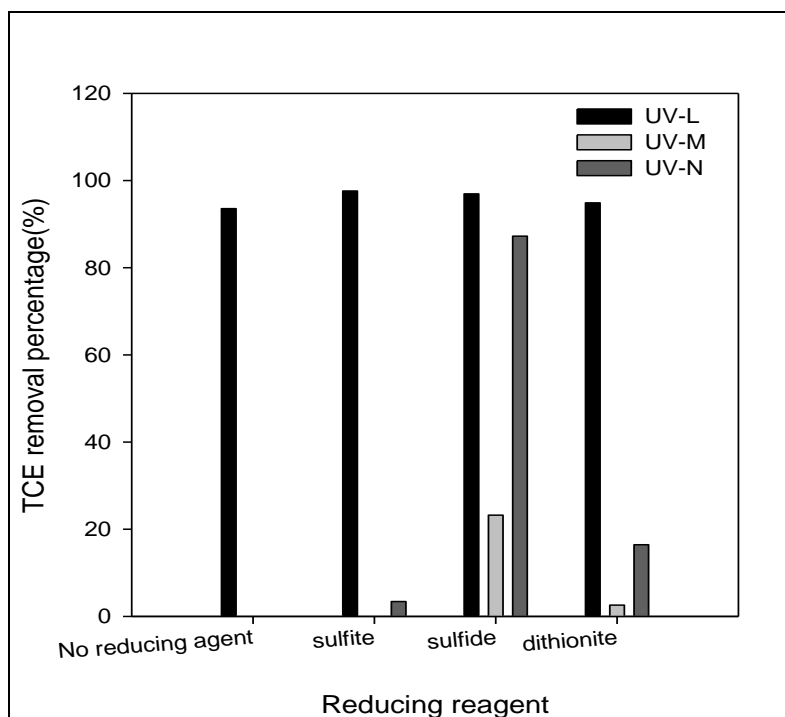


Figure 4.1: Screening experiments for TCE removal efficiency with different reagents and UV light sources. Experimental conditions: Initial TCE concentration= 0.23 mM, reducing agent concentration= 4.6 mM, Applied irradiation time= 3 h.

Dithionite absorb light at wavelength 315 nm and therefore if TCE degradation by dithionite were obtained as a result of radicals generated by dithionite irradiation, UV-N would have achieved high TCE removal efficiency because UV-N produces light at different wavelengths in the range of 280 – 320 nm wavelength including peaks near 312 nm. However, this was not the case indicating that the high removal efficiency obtained with UV-L/dithionite could be caused mainly by direct photolysis of TCE with UV-L and not by reactions with dithionite radicals.

Both UV-L/sulfide and UV-N/sulfide ARPs showed high TCE removal above 80% after 3 hours irradiation time. Bisulfide (HS^-) absorbs UV light with an absorption

peak at 230 nm,^{54, 55} and sulfide (S^{2-}) shows the absorption peak near 300 nm⁵⁴ while H_2S absorbs in the range of 210 – 270 nm.^{52, 55} High TCE removal with UV-N/sulfide could be caused by S^{2-} irradiation with UV-N and producing reducing radicals such as sulfide radicals or aqueous electrons since UV-N produces its light within the range of 280 – 320 nm with a peak at 312 nm wavelength which is near the wavelength of S^{2-} absorption.

When sulfite was used as reducing agent, significant TCE removal was obtained with UV-L and neither UV-N nor UV-M showed good removal. Since UV-L achieved high TCE removal efficiency with all screened reducing agents and the highest TCE removal efficiency was obtained with UV-L/sulfite ARP, this combination was selected for further investigation to obtain the optimum conditions for complete TCE degradation and maximum chloride recovery. Also UV-L is the most commonly used UV light type in water treatment applications (e.g. disinfection) because of its low energy requirements compared to UV-N and UV-M and therefore it is the most desirable activating method.

4.2. Characteristics of TCE degradation with UV-L/sulfite ARP

A set of kinetic experiments were conducted at different initial conditions (Table 4.2) to evaluate efficiency and rate of TCE degradation as affected by operating parameters. The purpose of these experiments was to identify the optimum conditions for TCE removal and to understand the removal mechanisms. The percentage of chloride recovery was used to evaluate effectiveness of ARP treatment process. The observed

degradation rate constant (k_{obs}) was calculated for each condition assuming pseudo-first-order decay to evaluate reaction rate according to the following equation:

$$C_{TCE} = C_{TCE_0} e^{-k_{obs}t} \quad (4.1)$$

where C_{TCE_0} is the initial molar concentration of TCE (mM), C_{TCE} is TCE concentration at irradiation time t (min), and k_{obs} is the pseudo-first-order rate constant (min^{-1}). Uncertainties represent 95% confidence limits expressed in % relative to estimate for k_{obs} .

The percentage of chloride recovery and k_{obs} for each batch test are presented in Table 4.2. Two control experiments were conducted to evaluate TCE loss due to volatilization or other mechanisms during the experiments and to evaluate TCE degradation by sulfite alone without UV irradiation. One control includes only TCE in water without any UV irradiation or sulfite and the other includes TCE and sulfite in water without UV irradiation. Results of control experiments showed that about 5.7% TCE was lost during the experimental and analytical procedures of TCE kinetic experiments. Sulfite alone in the absence of UV-L light removed about 7% of initial TCE concentration after 5 hours reaction time, which is the average value calculated from four batch tests. Chu and Jia have reported TCE loss through volatilization of about 10%.³¹ In this study, k_{obs} of TCE decay with UV-L/sulfite ARP was calculated without considering the loss due to volatility or by reaction with sulfite alone.

Table 4.2: Experimental conditions, calculated pseudo-first-order rate constants, and chloride recovery during TCE degradation by UV-L/Sulfite ARP.

No.	Initial TCE conc. (mM)	Sulfite dose (mM)	pH ^c	UV light intensity approx. ($\mu\text{W}/\text{cm}^2$)	k_{obs} ^a (1/min)	Chloride ion recovery (%)
Exp. 1	0.228	0	11	5000	0.015 ($\pm 5.9\%$) ^b	51.6
Exp. 2	0.228	0.46 (x2)	11	5000	0.029 ($\pm 9.1\%$)	65.1
Exp. 3	0.228	2.3 (x10)	11	5000	0.080 ($\pm 9.3\%$)	76.0
Exp. 4	0.228	4.6 (x20)	11	5000	0.136 ($\pm 3.3\%$)	83.5
Exp. 5	0.228	11.5 (x50)	11	5000	0.159 ($\pm 7.5\%$)	97.9
Exp. 6	0.0076	0.38 (x50)	9	5000	-	62.1
Exp. 7	0.076	3.8 (x50)	9	5000	0.193 ($\pm 30.4\%$)	72.5
Exp. 8	0.228	11.5 (x50)	9	5000	0.167 ($\pm 23.6\%$)	96.0
Exp. 9	0.38	19 (x50)	9	5000	0.120 ($\pm 14.5\%$)	83.6
Exp. 10	0.228	11.5 (x50)	7	5000	0.132 ($\pm 14.6\%$)	78.0
Exp. 11	0.228	11.5 (x50)	4	5000	0.016 ($\pm 14.8\%$)	-
Exp. 12	0.228	4.6 (x20)	11	3000	0.084 ($\pm 3.3\%$)	83.2
Exp. 13	0.228	4.6 (x20)	11	1000	0.031 ($\pm 6.8\%$)	46.2

^a k_{obs} was determined by a nonlinear-regression using MATLAB.

^b Uncertainties represent 95% confidence limits expressed in percentage relative to estimate for k_{obs} .

^c The pH is a nominal value and measured pH over time is presented in Table 4.3.

Table 4.3: pH changes over time during the kinetic experiments

Time (min) No.	0	30	60	90	120	180	240	300
Exp. 1	10.74	-	10.73	-	10.51	10.44	10.45	10.48
Exp. 2	10.97	-	10.64	-	10.68	10.73	10.52	10.66
Exp. 3	10.91	-	10.83	-	10.80	10.78	10.84	10.84
Exp. 4	10.77	-	10.75	-	10.80	10.83	10.90	10.87
Exp. 5	10.62	-	10.58	-	10.65	-	10.87	10.61
Exp. 6	8.87	-	8.40	-	8.08	7.88	7.78	7.75
Exp. 7	9.46	-	10.56	-	10.72	-	10.87	-
Exp. 8	9.55	-	10.14	-	10.48	-	10.77	-
Exp. 9	8.90	8.86	9.05	9.49	-	-	-	-
Exp. 10	7.82	-	7.84	-	7.97	-	8.57	-
Exp. 11	4.07	4.1	3.94	3.89	3.87	-	-	-

pH values were not measured for experiments 12 and 13.

Results shown in Table 4.2 indicate that increased chloride recovery was obtained at basic pH conditions. Also, increasing sulfite dose resulted in increasing chloride recovery at the same TCE initial concentration. Effects of different operating parameters on the kinetics and behavior of TCE degradation are described in the following sections.

4.2.1. Effect of sulfite dose on kinetics of TCE degradation

Figure 4.2 shows kinetics of TCE degradation at different sulfite doses with UV-L irradiation at pH ~11 and light intensity of ~5000 $\mu\text{W}/\text{cm}^2$. TCE degradation rates

were generally enhanced with increasing sulfite dose. However, at sulfite dose above 4.6 mM (20 times initial TCE concentration), no significant increase in the reaction rate was observed. TCE dechlorination can be caused either by the direct photolysis of TCE or by the free reducing radicals (sulfite radical or hydrated electron) produced from sulfite photolysis.³ In the absence of sulfite, TCE was removed with UV-L irradiation alone by the direct photolysis, showing the half-life time ($t_{1/2}$) of 48 min, as shown in Figure 4.2a. The solid lines in Figure 4.2a are the fitting non-linear regression model for the first order rate equation calculated using Matlab.

TCE absorbs UV light in the wavelength range of 200 – 250 nm.¹³ Chu and Jia reported the maximum absorption wavelength of TCE to be at 213 nm.³¹ In this study, TCE was completely degraded by UV-L in 5 hours by the direct photolysis in anaerobic environment, showing $k_{obs} = 0.014$ (1/min) with photon irradiance of 1.06×10^{-4} (Einstein/m²sec). Photon irradiance was calculated by converting the light intensity units from Joule/m²sec to Einstein/m²sec. This was done by dividing light intensity by the photon energy (hcN_A/λ) where N_A is the Avogadro's number (6.022×10^{23} 1/mol), h is Planck's constant (6.626×10^{-34} J.s), c is the speed of light (3×10^8 m/s), and λ is UV-L light wavelength (254 nm).

Chloride recovery for direct photolysis of TCE with UV-L was only 52% (Figure 4.2b) although TCE was completely degraded indicating that almost half of TCE concentration was converted to intermediate chlorinated products.

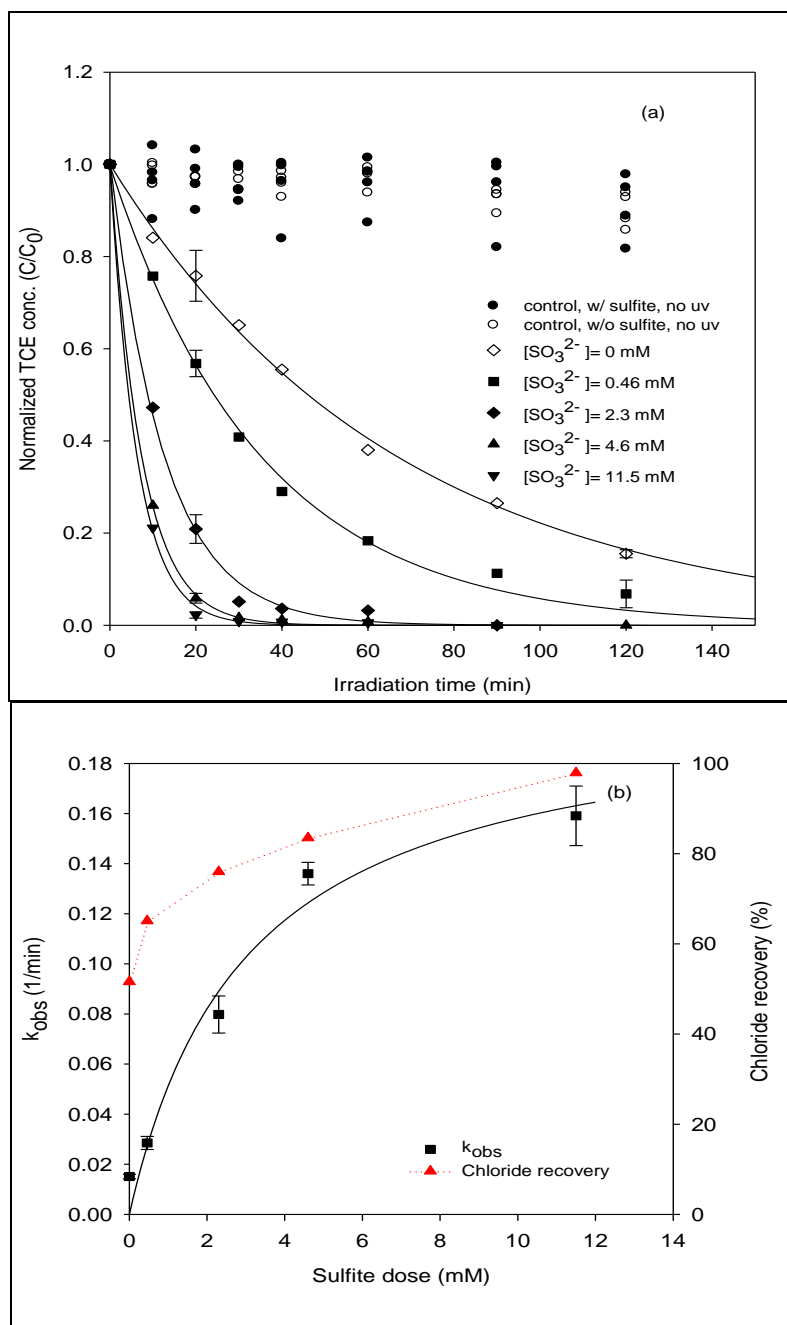
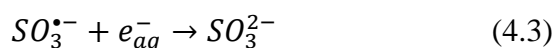
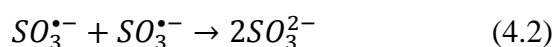


Figure 4.2: Effect of sulfite dose on TCE degradation. (a) Rate of TCE degradation with time (b) The pseudo-first-order rate constants and chloride recovery. Experimental conditions: initial TCE conc.= 0.23 mM, UV-L light intensity= $\sim 5000 \mu W/cm^2$, and pH ~ 11 . The solid line in (b) shows the predictions of k_{obs} by a saturation model: $k_{obs,predicted} = a \times C_{sulfite} / (b + C_{sulfite})$ where $a = 0.2060$ 1/min and $b = 3.0217$ mM.

The presence of sulfite enhanced TCE dechlorination rates indicating that reductant radicals produced by sulfite photolysis with UV-L contributed to TCE degradation. As sulfite dose is increased the amount of radicals formed increased and accordingly the degradation rate of TCE increased. At sulfite dose higher than 20 times the initial TCE concentration, the degradation rate did not increase much. Similar result was found in 1,2-DCA degradation by UV-L/sulfite ARP.³⁷ This could be explained by the sulfite radical recombination. When reductant radicals ($SO_3^{\bullet-}$) are produced with high amounts, they can recombine to form sulfite ion according to reactions described by Equations 4.2 and 4.3.



Chloride recovery continuously increased with increasing sulfite dose until it reached 97.7% at molar ratio of sulfite dose to initial TCE concentration of 50:1 (Figure 4.2b). This suggests that the excessive radicals produced were able to transform intermediate chlorinated products to chloride ion.

4.2.2. Effects of initial TCE concentration

Figure 4.3 presents the effect of initial TCE concentration on its degradation rate at pH ~9. The stoichiometric molar ratio of sulfite dose to initial TCE molar concentration was fixed at 50 times during these experiments. The TCE degradation rate slightly decreased with increasing initial TCE concentration. Chloride ion recovery showed the highest value of 96% at 0.23 mM initial TCE concentration whereas chloride

recovery decreased to 83.6% at higher initial concentration. This could be explained by the sulfite radical recombination at high sulfite doses as described before.

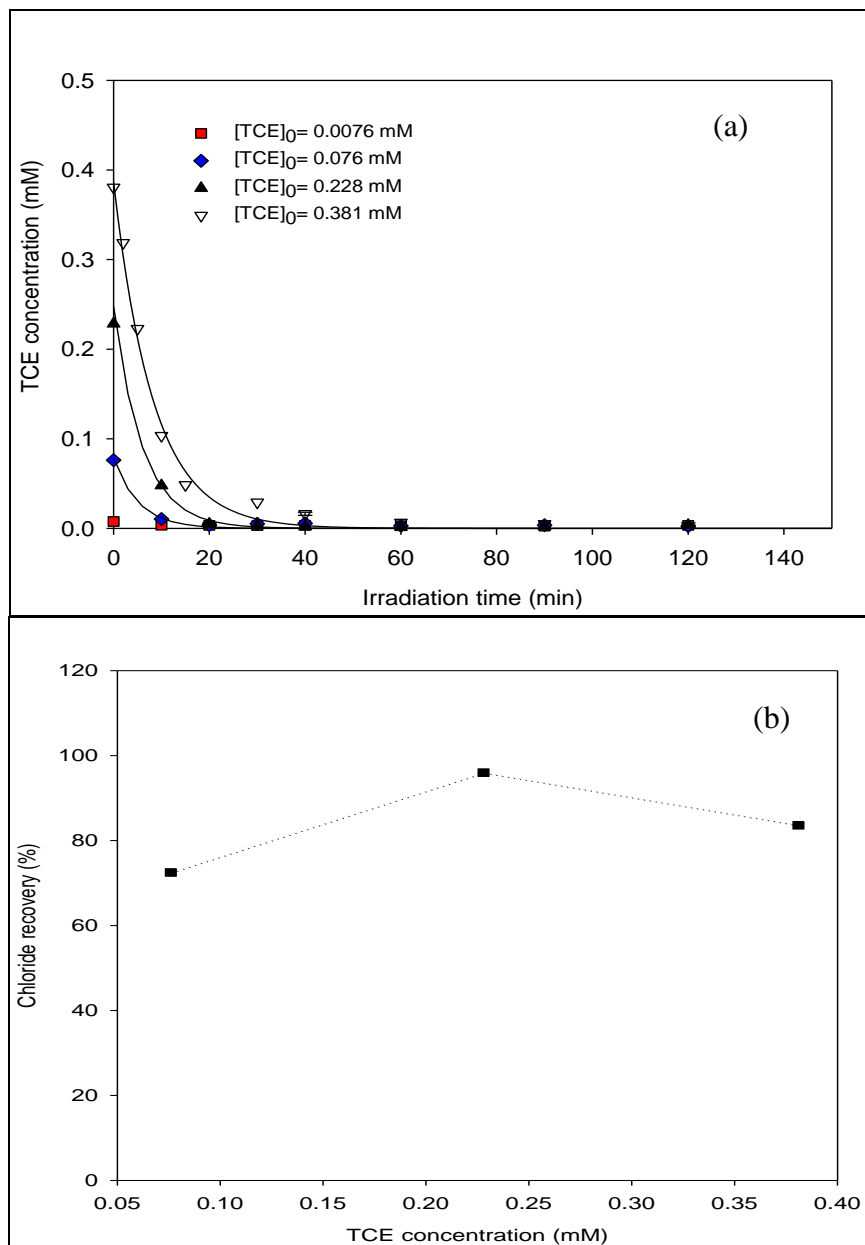


Figure 4.3: Effect of initial TCE concentration. (a) Rate of TCE degradation with time (b) Chloride recovery. Experimental conditions: The stoichiometric molar ratio of sulfite dose to initial TCE concentration was fixed at 50 times. UV-L light intensity= $\sim 5000 \mu\text{W}/\text{cm}^2$, and pH ~ 9

4.2.3. Effect of solution pH on TCE degradation kinetics

Effect of solution pH on TCE degradation kinetics was evaluated at initial TCE concentration of 0.23 mM, sulfite dose of 11.5 mM, and UV-L light intensity of $\sim 5000 \mu\text{W}/\text{cm}^2$. Batch experiments were conducted at four different initial pH values (pH 4, 7, 9, and 11; these are nominal values, refer to Table 4.3 for measured initial pH for each experiment). The changes of pH values over reaction time were presented earlier in Table 4.3. The pH was first adjusted to pH 7 using phosphate buffer as described in Chapter 3, then the desired pH value was obtained using HCl or NaOH solutions. Figure 4.4 shows the influence of solution pH on TCE degradation kinetics. TCE degradation rate was almost the same at neutral and basic conditions and almost complete TCE degradation was obtained within 20 minutes at these pH conditions. However, chloride recovery increased from 78% at pH ~ 7 to 96% at pH ~ 9 and 97.9% at pH ~ 11 . The high chloride recovery at basic pH conditions could be due to the fact that SO_3^- is the major sulfite species produced at basic pH which results in producing more sulfite radicals than neutral and acidic pH conditions. Vellanki et al. showed that light absorbance by sulfite solution at 254 nm wavelength increased with increasing pH except for very acidic conditions. He reported that the molar absorptivity at pH values of 2.5, 5.2, 7.5, 9.0, and 10.9 were 25.5, 7.6, 15.2, 17.4, and 18.2 ($\text{M}^{-1}\text{cm}^{-1}$), respectively.³⁹ The low and slow TCE degradation rate at pH ~ 4 confirms that UV-L light absorbance by sulfite at moderately acidic conditions was minimum.

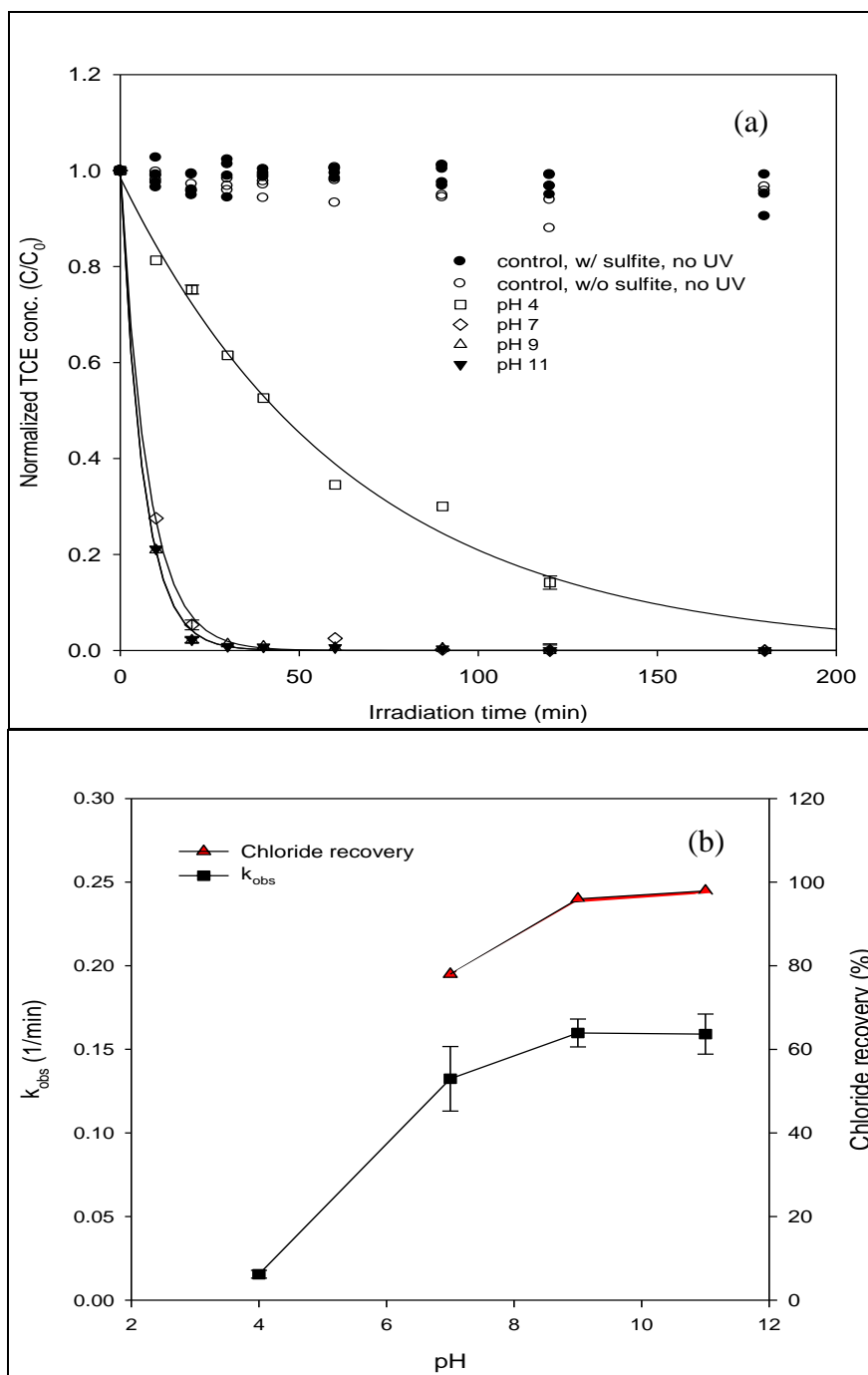


Figure 4.4: Effect of pH on TCE degradation. (a) Rate of TCE degradation with time (b) The pseudo-first-order rate constants and chloride recovery. Experimental conditions: initial TCE conc.= 0.23 mM, sulfite conc.= 11.5 mM, and UV-L light intensity= $\sim 5000 \mu\text{W}/\text{cm}^2$.

4.2.4. Effect of light intensity on Kinetics of TCE degradation

Effect of light intensity on efficiency and rate of TCE degradation was evaluated using three different light intensities (~ 1000 , ~ 3000 , and $\sim 5000 \mu\text{W}/\text{cm}^2$). Light intensity was controlled by varying the number of UV-L lamps used in these experiments where the light intensity of each lamp is approximately $1000 \mu\text{W}/\text{cm}^2$. Light intensity was measured using UVC 512 light meter (General Specialty Tools & Instruments). These experiments were conducted at pH ~ 11 but molar ratio of sulfite dose to initial TCE concentration of 20:1 which achieved less chloride recovery than 50:1 ratio. The purpose of using lower sulfite dose in this set of experiment is to investigate how light intensity can influence chloride recovery at moderate sulfite dose.

Effect of light intensity on TCE degradation kinetics is shown in Figure 4.5. TCE degradation rate increased with increasing light intensity and the rate constant (k_{obs}) increased linearly as the light intensity increased as shown in Figure 4.5b. This indicates that the production rate of reactive radicals increased with increasing UV irradiance which resulted in rapid TCE degradation. These results agree with the previous studies on both 1,2-DCA and VC by UV-L/sulfite ARPs.^{3,37} Chloride recovery increased as the light intensity increased from ~ 1000 to $\sim 3000 \mu\text{W}/\text{cm}^2$ and then remained constant as the light intensity increased from ~ 3000 to $\sim 5000 \mu\text{W}/\text{cm}^2$. This suggests that chloride recovery was controlled by sulfite dose and accordingly the amount of radicals that can convert TCE to chloride ion.

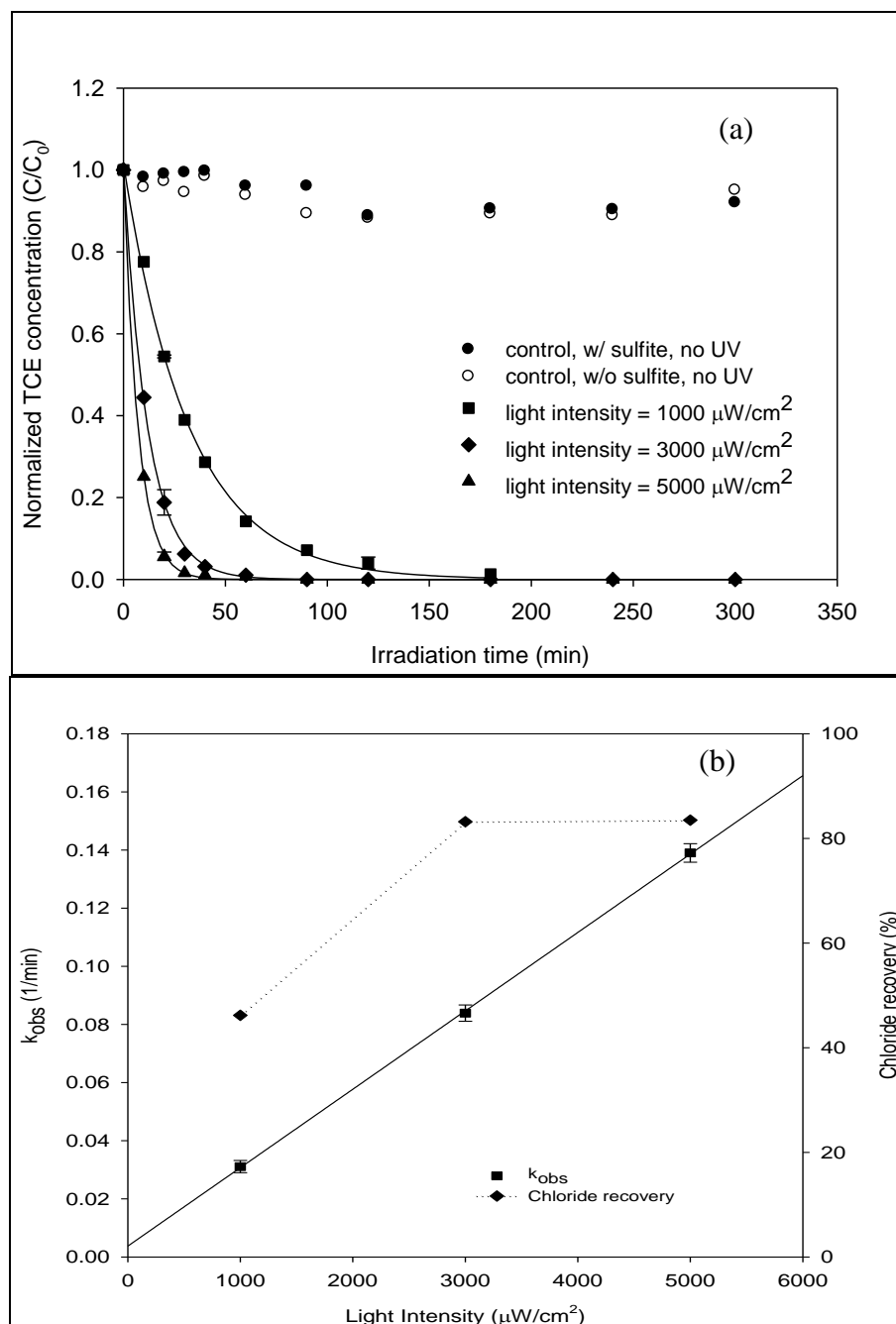


Figure 4.5: Effect of light intensity on TCE degradation. (a) Rate of TCE degradation with time (b) The pseudo-first-order rate constant and chloride recovery. Experimental conditions: initial TCE conc.= 0.23 mM, sulfite dose = 4.6 mM, and pH= ~11.

4.3. TCE degradation products

Results of kinetic experiments showed that chloride was the major final product from TCE degradation using UV-L/sulfite ARP approaching more than 97% when the ratio of sulfite dose to initial TCE concentration was 50:1 and light intensity was $\sim 5000 \mu\text{W}/\text{cm}^2$. Chloride recovery was calculated in this study using the following equation.

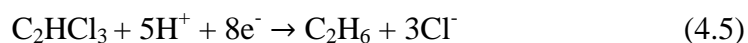
$$R = (C_{Cl, \text{ final chloride}})/(C_{Cl, \text{ in initial TCE}} - C_{Cl, \text{ in final TCE}}) \quad (4.4)$$

Where R is the chloride ion recovery (dechlorination efficiency), $C_{Cl, \text{ final chloride}}$ is the final chloride ion concentration (mM), $C_{Cl, \text{ in initial TCE}}$ and $C_{Cl, \text{ in final TCE}}$ are the chlorine concentrations (mM) in initial and final TCE respectively.

Direct photolysis of 0.23 mM TCE solution with UV-L light at light intensity of $\sim 5000 \mu\text{W}/\text{cm}^2$ in the absence of sulfite achieved only 51.6% chloride recovery. However, additions of sulfite greatly enhanced chloride recovery. At sulfite dose of 11.5 mM (50 times TCE initial concentration) and light intensity of $\sim 5000 \mu\text{W}/\text{cm}^2$, chloride recoveries were 95.9 % and 97.8% at pH ~ 9 and pH ~ 11 , respectively.

An attempt was made to identify intermediate by-products and final products other than chloride especially for conditions that did not achieve high chloride removal. The purpose of this task was to try to understand TCE degradation pathway and reaction mechanisms. GC-MS was used to quantify chlorinated by-products that could be formed in this system. When TCE concentration was 0.23 mM and sulfite dose was 4.6 mM at pH ~ 11 , samples were taken after 5 min, 20 min, and 120 min irradiation time and were analyzed using GC-MS. No peaks of chlorinated products were found in these samples. Chloride ion recovery in 120 min irradiation time in this experiment was 83.5%. This

implies that 16.5% of initial chlorine (5.5% of initial TCE) was lost. This could be due to the formation of products that were not detected by GC-MS or volatile products that were lost by volatilization. The difference could also be due to experimental errors in quantifying TCE concentrations. A possible reaction pathway of TCE degradation can be by the following equation which was also suggested by Parshetti and Doong;²⁹



Ethane formation including ethane and acetylene was not confirmed in this study, it was remained for a further study.

One experiment was conducted at high initial TCE concentration of 1 mM in order to check by-products which were not detected at low TCE concentration. Monochloroacetylene, dichloroacetylene (DCA), and cis-DCE were detected with very small peaks after 2 hours irradiation with UV-L. Figure 4.6 shows the by-product peaks obtained from GC-MS chromatogram. The total retention time was 18 min but the three chlorinated products were found in the first 3 minutes before the hexane peak.

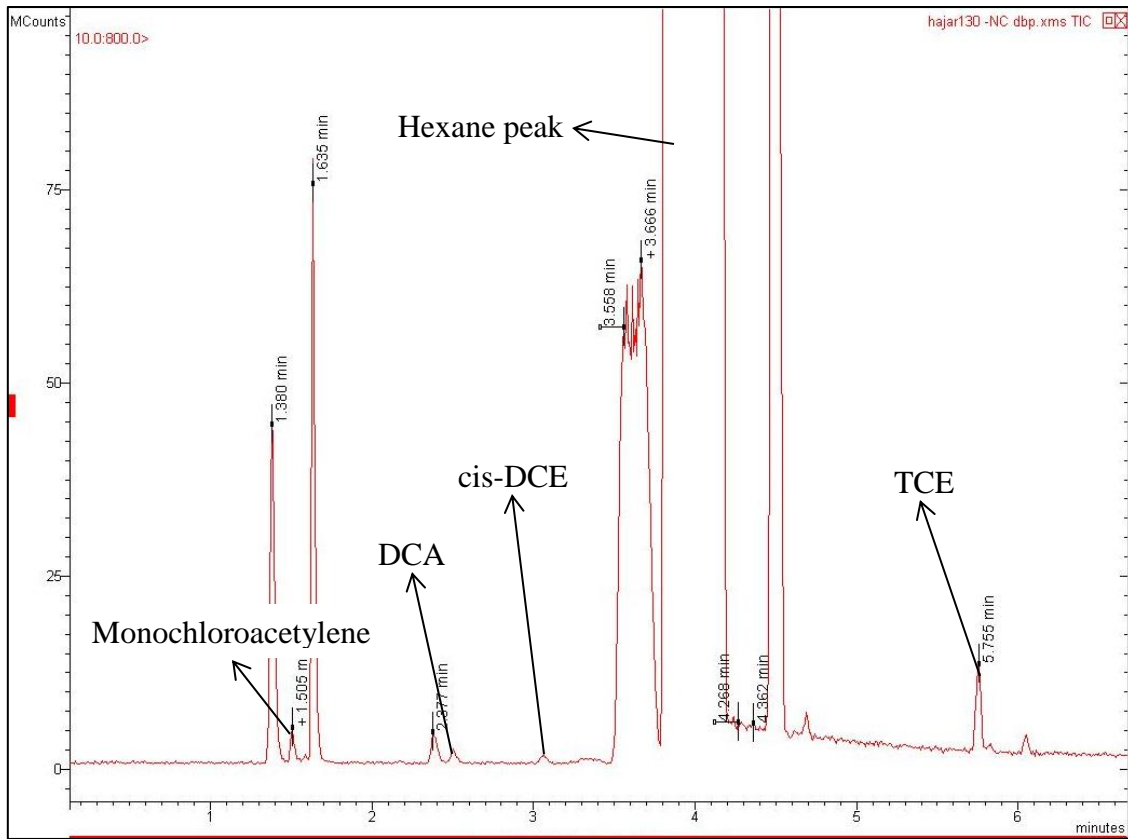


Figure 4.6: Chlorinated by-product peaks detected by GC-MS

5. CONCLUSION

This study investigated the degradation of trichloroethylene (TCE) using advanced reduction processes (ARPs). Screening experiments were performed using combinations of sulfite, sulfide, and dithionite as reducing agents and UV-L, UV-M, and UV-N activating methods. The screening test results showed the highest removal (97.6%) using the combination of sulfite and UV-L. This ARP was used to investigate the effect of different process variables (TCE initial concentration, sulfite dose, solution pH, and light intensity) on TCE degradation rates.

The specific conclusions from this study can be summarized as follows:

1. Screening experiments showed that UV-L generally is successful to degrade TCE, regardless of reducing reagents, indicating that TCE is degraded by direct photolysis but not completely to chloride ion in this case.
2. The ARP that combines sulfite with UV-L provides the most effective TCE removal.
3. The optimum condition was found when sulfite dose was 50 times initial TCE concentration, light intensity of $\sim 5000 \mu\text{W}/\text{cm}^2$, and alkaline pH conditions.
4. Generally higher pH leads to faster TCE degradation and this is due to the production of reactive sulfite species at high pH.
5. Increasing sulfite dose resulted in increasing the rate of TCE dechlorination.

6. UV light intensity resulted in linear increase in the pseudo-first-order rate constant.
7. Higher light intensities result in faster loss of sulfite. Limited increase in chloride recovery with increasing light intensity from $\sim 3000 \mu\text{W}/\text{cm}^2$ to $\sim 5000 \mu\text{W}/\text{cm}^2$ indicates that the rate was controlled by sulfite dose.
8. Finally, application of ARPs in treatment systems is promising to degrade TCE rapidly and completely.

REFERENCES

- (1) Yu, H.; Nie, E.; Xu, J.; Yan, S.; Cooper, W. J.; Song, W. Degradation of diclofenac by advanced oxidation and reduction processes: kinetic studies, degradation pathways and toxicity assessments. *Water Res.* **2013**, *47*, 1909-1918.
- (2) Deng, Y.; Ezyske, C. M. Sulfate radical-advanced oxidation process (SR-AOP) for simultaneous removal of refractory organic contaminants and ammonia in landfill leachate. *Water Res.* **2011**, *45*, (18), 6189-6194.
- (3) Liu, X.; Yoon, S.; Batchelor, B.; Abdel-Wahab, A. Degradation of vinyl chloride (VC) by the sulfite/UV advanced reduction process (ARP): effects of process variables and kinetic model. *Sci. Total Environ.* **2013**, *454-455*, 578-583.
- (4) Vellanki, B. P.; Batchelor, B.; Abdel-Wahab, A. Advanced reduction processes: a new class of treatment processes. *Environ. Eng. Sci.* **2013**, *30*, (5), 264-271.
- (5) Yoon, S. H.; Abdel-Wahab, A.; Batchelor, B. In *Advanced reduction processes for hazardous waste treatment*, Qatar Foundation Annual Research Forum Proceedings, Doha, **2011**; EVP16.
- (6) Burris, D. R.; Delcomyn, C. A.; Deng, B.; Buck, L. E.; Hatfield, K. Kinetics of tetrachloroethylene-reductive dechlorination catalyzed by vitamin B₁₂. *Environ. Toxicol. Chem.* **1998**, *17*, (9), 1681-1688.
- (7) United States Environmental Protection Agency (EPA), 2007; <http://www.epa.gov/ttnatw01/hlthef/tri-ethy.html>. (Accessed 2013, October 13).

- (8) Code of federal regulations (annual edition), 2013;
<http://www.gpo.gov/fdsys/pkg/CFR-2013-title40-vol28/pdf/CFR-2013-title40-vol28-part268.pdf>. (Accessed 2014, March 13).
- (9) Chawla, R. C.; Doura, K. F.; McKay, D. In *Effect of alcohol cosolvents on the aqueous solubility of trichloroethylene*, Conference on Environmental Research, **2001**.
- (10) Russell, R. B.; Breed, J.; Barton, G. J. Conservation analysis and structure prediction of the SH₂ family of phosphotyrosine binding domains. *Fed. Eur. Biochem. Soc.* **1992**, *304*, (1), 15-20.
- (11) Miller, R. S.; Khan, Z.; Doty, S. L. Comparison of trichloroethylene toxicity, removal, and degradation by varieties of populus and salix for improved phytoremediation applications. *J. Bioremed. Biodeg.* **2011**, *S7*.
- (12) Dobaradaran, S.; Nabizadeh, R.; Mahvi, A. H.; Noroozi, A.; Yunesian, M.; Rastkari, N.; Nazmara, S.; Zarei, S. Kinetic and degradation efficiency of trichloroethylene (TCE) via photochemical process from contaminated water. *Afr. J. Biotechnol.* **2012**, *11*, (8), 2006-2012.
- (13) Li, K.; Stefan, M. I.; Crittenden, J. C. UV photolysis of trichloroethylene: product study and kinetic modeling. *Environ. Sci. Technol.* **2004**, *38*, 6685-6693.
- (14) Tao, T.; Yang, J. J.; Maciel, G. E. Photoinduced decomposition of trichloroethylene on soil components. *Environ. Sci. Technol.* **1999**, *33*, 74-80.
- (15) Sun, Y.; Brown, G. M.; Moyer, B. A. TiO₂ mediated photooxidation of trichloroethylene and toluene dissolved in fluorocarbon solvents. *Chemosphere* **1995**, *31*, (6), 3575-3584.

- (16) Liu, H.; Cheng, S. a.; Zhang, J.; Cao, C.; Jiang, W. The gas-photocatalytic degradation of trichloroethylene without water. *Chemosphere* **1997**, *35*, (12), 2881-2889.
- (17) Keshmiri, M.; Troczynski, T.; Mohseni, M. Oxidation of gas phase trichloroethylene and toluene using composite sol-gel TiO₂ photocatalytic coatings. *J. Hazard. Mater. B* **2006**, *128*, 130-137.
- (18) Ou, H.-H.; Lo, S.-L. Photocatalysis of gaseous trichloroethylene (TCE) over TiO₂: the effect of oxygen and relative humidity on the generation of dichloroacetyl chloride (DCAC) and phosgene. *J. Hazard. Mater.* **2007**, *146*, 302-308.
- (19) Tanimura, T.; Yoshida, A.; Yamazaki, S. Reduced formation of undesirable by-products from photocatalytic degradation of trichloroethylene. *Appl. Catal., B* **2005**, *61*, 346-351.
- (20) Guo-Min, Z.; Zhen-Xing, C.; Min, X.; Xian-Qing, Q. Study on the gas-phase photolytic and photocatalytic oxidation of trichloroethylene. *J. Photochem. Photobiol., A* **2003**, *161*, 51-56.
- (21) Amama, P. B.; Itoh, K.; Murabayashi, M. Photocatalytic degradation of trichloroethylene in dry and humid atmospheres: role of gas-phase reactions. *J. Mol. Catal. A: Chem.* **2004**, *217*, 109-115.
- (22) Shen, Y.-S.; Ku, Y.; Ma, C.-M. Reflection effect on the decomposition of gas-phase trichloroethene by 254 nm UV photolysis and advanced oxidation processes (AOPs). *Sustain. Environ. Res.* **2012**, *22*, (6), 401-411.
- (23) Adhikari, D. L.; Sato, C.; Lamichhane, S. K. Contamination of trichloroethylene in drinking water system and its degradation. *The Himalayan Physics* **2012**, *3*, 13-17.

- (24) Buechler, K. J.; Noble, R. D.; Koval, C. A.; Jacoby, W. A. Investigation of the effects of controlled periodic illumination on the oxidation of gaseous trichloroethylene using a thin film of TiO₂. *Ind. Eng. Chem. Res.* **1999**, *38*, 892-896.
- (25) Weir, B. A.; Sundstorm, D. W. Destruction of trichloroethylene by UV light-catalyzed oxidation with hydrogen peroxide. *Chemosphere* **1993**, *27*, (7), 1279-1291.
- (26) Wang, D.; Bolton, J. R.; Hofmann, R. Medium pressure UV combined with chlorine advanced oxidation for trichloroethylene destruction in a model water. *Water Res.* **2012**, *46*, 4677-4686.
- (27) Dobaradaran, S.; Lutze, H.; Mahvi, A. H.; Schmidt, T. C. Transformation efficiency and formation of transformation products during photochemical degradation of TCE and PCE at micromolar concentrations. *Iranian J. Environ. Health Sci. Eng.* **2014**, *12*, (16).
- (28) Parshetti, G. K.; Doong, R.-a. Synergistic effect of nickel ions on the coupled dechlorination of trichloroethylene and 2,4-dichlorophenol by Fe/TiO₂ nanocomposites in the presence of UV light under anoxic conditions. *Water Res.* **2011**, *45*, 4198-4210.
- (29) Parshetti, G. K.; Doong, R.-a. Dechlorination and photodegradation of trichloroethylene by Fe/TiO₂ nanocomposites in the presence of nickel ions under anoxic conditions. *Appl. Catal., B* **2010**, *100*, 116-123.
- (30) Joo, J. C.; Ahn, C. H.; Jang, D. G.; Yoon, Y. H.; Kim, J. K.; Campos, L.; Ahn, H. Photocatalytic degradation of trichloroethylene in aqueous phase using nano-ZnO/Laponite composites. *J. Hazard. Mater.* **2013**, *263*, 569-574.

- (31) Chu, W.; Jia, J. The photodegradation and modeling of a typical NAPL, trichloroethene, by monochromatic UV irradiations. *Environ. Sci. Technol.* **2009**, *43*, 1455-1459.
- (32) Mertens, R.; Sonntag, C. v. Photolysis ($\lambda=254$ nm) of tetrachloroethene in aqueous solutions. *J. Photochem. Photobiol., A* **1995**, *85*, 1-9.
- (33) Mohseni, M. Gas phase trichloroethylene (TCE) photooxidation and byproduct formation: photolysis vs. titania/silica based photocatalysis. *Chemosphere* **2005**, *59*, 335-342.
- (34) Gantzer, C. J.; Wackett, L. P. Reductive dechlorination catalyzed by bacterial transition-metal coenzymes. *Environ. Sci. Technol.* **1991**, *25*, 715-722.
- (35) Burris, D. R.; Delcomyn, C. A.; Smith, M. H.; Roberts, A. L. Reductive dechlorination of tetrachloroethylene and trichloroethylene catalyzed by vitamin B₁₂ in homogeneous and heterogeneous systems. *Environ. Sci. Technol.* **1996**, *30*, 3047-3052.
- (36) Yoon, S.; Han, D. S.; Liu, X.; Batchelor, B.; Abdel-Wahab, A. Degradation of 1,2-dichloroethane using advanced reduction processes. *J. Environ. Chem. Eng.* **2014**, *2*, 731-737.
- (37) Liu, X.; Vellanki, B. P.; Batchelor, B.; Abdel-Wahab, A. Degradation of 1,2-dichloroethane with advanced reduction processes (ARPs): effects of process variables and mechanisms. *Chem. Eng. J.* **2014**, *237*, 300-307.
- (38) Bensalah, N.; Nicola, R.; Abdel-Wahab, A. Nitrate removal from water using UV-M/S₅O₄²⁻ advanced reduction process. *Int. J. Environ. Sci. Tech.* **2013**.

- (39) Vellanki, B. P.; Batchelor, B. Perchlorate reduction by the sulfite/ultraviolet light advanced reduction process. *J. Hazard. Mater.* **2013**, *262*, 348-356.
- (40) Liu, X.; Yoon, S.; Batchelor, B.; Abdel-Wahab, A. Photochemical degradation of vinyl chloride with an advanced reduction process (ARP) - effects of reagents and pH. *Chem. Eng. J.* **2013**, *215-216*, 868-875.
- (41) Bensalah, N.; Liu, X.; Abdel-Wahab, A. Bromate reduction by ultraviolet light irradiation using medium pressure lamp. *Int. J. Environ. Stud.* **2013**, *70*, (4), 566-582.
- (42) UV information; <http://www.emperoraquatics.com/uv-lamp-technologies.php>. (Accessed 2013, October 24).
- (43) Liu, X. Degradation of vinyl chloride and 1,2-dichloroethane by advanced reduction processes. Texas A&M University, 2013.
- (44) Song, Z.; Tang, H.; Wang, N.; Zhu, L. Reductive defluorination of perfluorooctanoic acid by hydrated electrons in a sulfite-mediated UV photochemical system. *Journal of hazardous materials* **2013**, *262*, 332-338.
- (45) Mayhew, S. G. The redox potential of dithionite and SO_2^- from equilibrium reactions with flavodoxins, methyl viologen and hydrogen plus hydrogenase. *Eur. J. Biochem.* **1978**, *85*, 535-547.
- (46) Amonette, J. E.; Szecsody, J. E.; Schaef, H. T.; Templeton, J. C.; Gorby, Y. A.; Fruchter, J. S., Abiotic reduction of aquifer materials by dithionite: a promising in-situ remediation technology. In *Thirty-Third Symposium on Health & the Environment In Situ Remediation: Scientific Base for Current & Future Technologies*, Richland, Washington, **1994**.

- (47) Hara, K.; Sayama, K.; Arakawa, H. UV photoinduced reduction of water to hydrogen in Na₂S, Na₂SO₃, and Na₂S₂O₄ aqueous solutions. *J. Photochem. Photobiol., A* **1999**, *128*, (1-3), 27-31.
- (48) Li, X.; Ma, J.; Liu, G.; Fang, J.; Yue, S.; Guan, Y.; Chen, L.; Liu, X. Effective reductive dechlorination of monochloroacetic acid by sulfite/UV process. *Environmental Science & Technology* **2012**, *46*, 7342-7349.
- (49) Buxton, G. V.; Greenstock, C. L.; Helman, W. P.; Ross, A. B. Critical review of rate constants for reactions of hydrated electrons, hydrogen atoms and hydroxyl radicals ($\bullet\text{OH}/\bullet\text{O}^{\cdot}$) in aqueous solution. *Phys. Chem. Ref. Data* **1988**, *17*, 513-886.
- (50) Christian Brandt; Eldik, R. v. Transition metal-catalyzed oxidation of sulfur (IV) oxides atmospheric-relevant processes and mechanisms. *Chem. Rev.* **1995**, *95*, 119-190.
- (51) Vellanki, B. P.; Batchelor, B. Perchlorate reduction by the sulfite/ultraviolet light advanced reduction process. *Journal of Hazardous Materials* **2013**, *262*, 348-356.
- (52) Linkous, C. A.; Huang, C.; Fowler, J. R. UV photochemical oxidation of aqueous sodium sulfide to produce hydrogen and sulfur. *J. Photochem. Photobiol., A* **2004**, *168*, 153-160.
- (53) Khriachtchev, L.; Pettersson, M.; Isoniemi, E.; Rasanen, M. 193 nm photolysis of H₂S in rare-gas matrices: luminescence spectroscopy of the products. *J. Chem. Phys.* **1998**, *108*, 5747-5754.
- (54) Piché, S.; Larachi, F. Dynamics of pH on the oxidation of HS⁻ with iron (III) chelates in anoxic conditions. *Chem. Eng. Sci.* **2006**, *61*, 7673-7683.

(55) Guenther, E. A.; Johnson, K. S.; Coale, K. H. Direct ultraviolet spectrophotometric determination of total sulfide and iodide in natural waters. *Anal. Chem.* **2001**, *73*, (14), 3481-3487.

(56) Neta, P.; Huie, R. E. Free-radical chemistry of sulfite. *Environ. Health Perspect.* **1985**, *64*, 209-217.